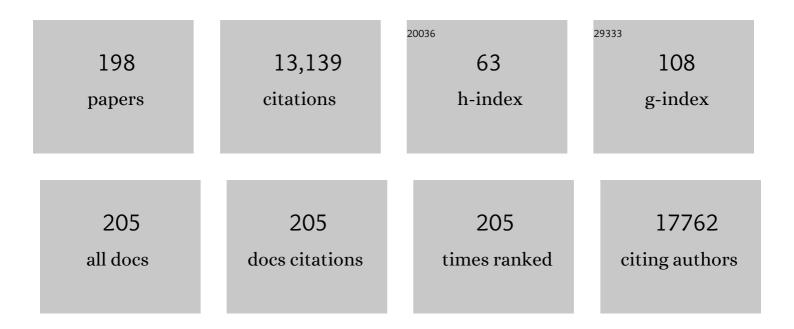
## Lifeng Liu

List of Publications by Year in descending order

Source: https://exaly.com/author-pdf/8489435/publications.pdf Version: 2024-02-01



LIEENC LU

#	Article	IF	CITATIONS
1	Lithium and sodium storage performance of tin oxyphosphate anode materials. Applied Surface Science, 2022, 579, 152126.	3.1	4
2	Iron Nanoparticles Confined in Periodic Mesoporous Organosilicon as Nanoreactors for Efficient Nitrate Reduction. ACS Applied Nano Materials, 2022, 5, 5149-5157.	2.4	9
3	Boosting acidic water oxidation performance by constructing arrays-like nanoporous IrxRu1â^xO2 with abundant atomic steps. Nano Research, 2022, 15, 5933-5939.	5.8	25
4	Single-atom Ir and Ru anchored on graphitic carbon nitride for efficient and stable electrocatalytic/photocatalytic hydrogen evolution. Applied Catalysis B: Environmental, 2022, 310, 121318.	10.8	72
5	Transition metal tellurides as emerging catalysts for electrochemical water splitting. Current Opinion in Electrochemistry, 2022, 34, 101031.	2.5	12
6	lridium–Iron Diatomic Active Sites for Efficient Bifunctional Oxygen Electrocatalysis. ACS Catalysis, 2022, 12, 9397-9409.	5.5	47
7	Multimetallic transition metal phosphide nanostructures for supercapacitors and electrochemical water splitting. Nanotechnology, 2022, 33, 432004.	1.3	11
8	Highly Efficient and Stable Saline Water Electrolysis Enabled by Selfâ€Supported Nickelâ€Iron Phosphosulfide Nanotubes With Heterointerfaces and Underâ€Coordinated Metal Active Sites. Advanced Functional Materials, 2022, 32, .	7.8	60
9	Amorphous phosphatized ruthenium-iron bimetallic nanoclusters with Pt-like activity for hydrogen evolution reaction. Applied Catalysis B: Environmental, 2021, 283, 119583.	10.8	78
10	Easy preparation of multifunctional ternary PdNiP/C catalysts toward enhanced small organic molecule electro-oxidation and hydrogen evolution reactions. Journal of Energy Chemistry, 2021, 58, 256-263.	7.1	31
11	Rhodium single-atom catalysts with enhanced electrocatalytic hydrogen evolution performance. New Journal of Chemistry, 2021, 45, 5770-5774.	1.4	13
12	Multifunctional Noble Metal Phosphide Electrocatalysts for Organic Molecule Electro-Oxidation. ACS Applied Energy Materials, 2021, 4, 1593-1600.	2.5	12
13	Atomic-Step Enriched Ruthenium–Iridium Nanocrystals Anchored Homogeneously on MOF-Derived Support for Efficient and Stable Oxygen Evolution in Acidic and Neutral Media. ACS Catalysis, 2021, 11, 3402-3413.	5.5	87
14	Efficient Bipolar Membrane Water Electrolysis Enabled By Dual-Phase CoP-CoTe2 Nanowires As Bifunctional Electrocatalyst. ECS Meeting Abstracts, 2021, MA2021-01, 2069-2069.	0.0	0
15	Multifunctional Noble Metal Phosphide Electrocatalysts for the Organic Molecule Electro-Oxidation. ECS Meeting Abstracts, 2021, MA2021-01, 2073-2073.	0.0	0
16	Ruthenium-Iridium Nanocrystals Anchored Homogeneously on MOF-Derived Support for Efficient and Stable Oxygen Evolution in Acidic and Neutral Media. ECS Meeting Abstracts, 2021, MA2021-01, 2059-2059.	0.0	0
17	Novel Quasi-Liquid K-Na Alloy as a Dendrite-Free Anode for Potassium Metal Batteries. ECS Meeting Abstracts, 2021, MA2021-01, 2071-2071.	0.0	0
18	Ultrafine Oxygen-Defective Iridium Oxide Nanoclusters for Efficient and Durable Water Oxidation at High Current Densities in Acidic Media. ECS Meeting Abstracts, 2021, MA2021-01, 2060-2060.	0.0	0

#	Article	lF	CITATIONS
19	Atomically Dispersed Ruthenium-Based Multifunctional Electrocatalysts for Efficient Overall Water Electrolysis Assisted By a Bipolar Membrane. ECS Meeting Abstracts, 2021, MA2021-01, 2082-2082.	0.0	0
20	Novel Quasiâ€Liquid Kâ€Na Alloy as a Promising Dendriteâ€Free Anode for Rechargeable Potassium Metal Batteries. Advanced Science, 2021, 8, e2101866.	5.6	18
21	Plasma tailoring in WTe2 nanosheets for efficiently boosting hydrogen evolution reaction. Journal of Materials Science and Technology, 2021, 78, 170-175.	5.6	23
22	Dual-phase CoPâ^'CoTe2 nanowires as an efficient bifunctional electrocatalyst for bipolar membrane-assisted acid-alkaline water splitting. Chemical Engineering Journal, 2021, 420, 130454.	6.6	52
23	Lithium–copper alloy embedded in 3D porous copper foam with enhanced electrochemical performance toward lithium metal batteries. Materials Today Energy, 2021, 22, 100871.	2.5	11
24	Exceptional lithium storage performance achieved by iron-based nanostructures upon extended high-rate cycling. Journal of Alloys and Compounds, 2021, 888, 161626.	2.8	4
25	Efficient hydrogen production by saline water electrolysis at high current densities without the interfering chlorine evolution. Journal of Materials Chemistry A, 2021, 9, 22248-22253.	5.2	35
26	Platinum group metal free nano-catalysts for proton exchange membrane water electrolysis. Current Opinion in Chemical Engineering, 2021, 34, 100743.	3.8	23
27	Light-driven oxygen evolution from water oxidation with immobilised TiO2 engineered for high performance. Scientific Reports, 2021, 11, 21306.	1.6	8
28	Bi-metallic cobalt-nickel phosphide nanowires for electrocatalysis of the oxygen and hydrogen evolution reactions. Catalysis Today, 2020, 358, 196-202.	2.2	46
29	Proteomic and Metabolic Elucidation of Solar-Powered Biomanufacturing by Bio-Abiotic Hybrid System. CheM, 2020, 6, 234-249.	5.8	60
30	Bamboo-like nitrogen-doped carbon nanotubes encapsulated with NiFeP nanoparticles and their efficient catalysis in the oxygen evolution reaction. Electrochimica Acta, 2020, 331, 135360.	2.6	23
31	Discovery of Realâ€Space Topological Ferroelectricity in Metallic Transition Metal Phosphides. Advanced Materials, 2020, 32, e2003479.	11.1	13
32	Ultrafine oxygen-defective iridium oxide nanoclusters for efficient and durable water oxidation at high current densities in acidic media. Journal of Materials Chemistry A, 2020, 8, 24743-24751.	5.2	45
33	Decoding of Oxygen Network Distortion in a Layered High-Rate Anode by <i>In Situ</i> Investigation of a Single Microelectrode. ACS Nano, 2020, 14, 11753-11764.	7.3	10
34	Nitrogen Doping Improves the Immobilization and Catalytic Effects of Co <sub>9</sub> S <sub>8</sub> in Li‣ Batteries. Advanced Functional Materials, 2020, 30, 2002462.	7.8	86
35	Bifunctional Porous Cobalt Phosphide Foam for High-Current-Density Alkaline Water Electrolysis with 4000-h Long Stability. ACS Sustainable Chemistry and Engineering, 2020, 8, 10193-10200.	3.2	57
36	Stable overall water splitting in an asymmetric acid/alkaline electrolyzer comprising a bipolar membrane sandwiched by bifunctional cobaltâ€nickel phosphide nanowire electrodes. , 2020, 2, 646-655.		79

#	Article	lF	CITATIONS
37	Strong Electronic Coupling between Ultrafine Iridium–Ruthenium Nanoclusters and Conductive, Acid-Stable Tellurium Nanoparticle Support for Efficient and Durable Oxygen Evolution in Acidic and Neutral Media. ACS Catalysis, 2020, 10, 3571-3579.	5.5	122
38	Strategies for Semiconductor/Electrocatalyst Coupling toward Solarâ€Driven Water Splitting. Advanced Science, 2020, 7, 1902102.	5.6	110
39	Ultrafine-Grained Porous Ir-Based Catalysts for High-Performance Overall Water Splitting in Acidic Media. ACS Applied Energy Materials, 2020, 3, 3736-3744.	2.5	26
40	Mille-Crêpe-like Metal Phosphide Nanocrystals/Carbon Nanotube Film Composites as High-Capacitance Negative Electrodes in Asymmetric Supercapacitors. ACS Applied Energy Materials, 2020, 3, 4580-4588.	2.5	19
41	Self-Epitaxial Hetero-Nanolayers and Surface Atom Reconstruction in Electrocatalytic Nickel Phosphides. ACS Applied Materials & amp; Interfaces, 2020, 12, 21616-21622.	4.0	9
42	One-step fabrication of a self-supported Co@CoTe <sub>2</sub> electrocatalyst for efficient and durable oxygen evolution reactions. Inorganic Chemistry Frontiers, 2020, 7, 2523-2532.	3.0	37
43	Nickel Phosphide Nanomaterials for Hydrogen Evolution Reaction. ECS Meeting Abstracts, 2020, MA2020-02, 1429-1429.	0.0	0
44	Synthesis and Characterization of Ordered Cobalt Phosphide Nanowire Arrays As a Potential Catalyst for HER/Oer Reactions ECS Meeting Abstracts, 2020, MA2020-02, 1433-1433.	0.0	0
45	General Synthetic Strategy for Pomegranate-like Transition-Metal Phosphides@N-Doped Carbon Nanostructures with High Lithium Storage Capacity. , 2019, 1, 265-271.		35
46	Inverted Pyramid Textured p-Silicon Covered with Co <sub>2</sub> P as an Efficient and Stable Solar Hydrogen Evolution Photocathode. ACS Energy Letters, 2019, 4, 1755-1762.	8.8	35
47	High-Performance Flexible Solid-State Asymmetric Supercapacitors Based on Bimetallic Transition Metal Phosphide Nanocrystals. ACS Nano, 2019, 13, 10612-10621.	7.3	214
48	The oxygen evolution reaction enabled by transition metal phosphide and chalcogenide pre-catalysts with dynamic changes. Chemical Communications, 2019, 55, 8744-8763.	2.2	246
49	Large-Scale Fabrication of Hollow Pt <sub>3</sub> Al Nanoboxes and Their Electrocatalytic Performance for Hydrogen Evolution Reaction. ACS Sustainable Chemistry and Engineering, 2019, 7, 9842-9847.	3.2	14
50	Artificial electrode interfaces enable stable operation of freestanding anodes for high-performance flexible lithium ion batteries. Journal of Materials Chemistry A, 2019, 7, 14097-14107.	5.2	21
51	Polyvinylpyrrolidone-Assisted Hydrothermal Synthesis of CuCoO <sub>2</sub> Nanoplates with Enhanced Oxygen Evolution Reaction Performance. ACS Sustainable Chemistry and Engineering, 2019, 7, 1493-1501.	3.2	48
52	Conformal and Continuous Deposition of Bifunctional Cobalt Phosphide Layers on p-Silicon Photocathodes for Improved Solar Hydrogen Evolution. ECS Meeting Abstracts, 2019, , .	0.0	1
53	Compositional and Microstructural Engineering of Transition Metal Phosphides for Improved Electrocatalytic Performance. ECS Meeting Abstracts, 2019, , .	0.0	0
54	Rationally engineered amorphous TiOx/Si/TiOx nanomembrane as an anode material for high energy lithium ion battery. Energy Storage Materials, 2018, 12, 23-29.	9.5	38

#	Article	IF	CITATIONS
55	Trends in activity for the oxygen evolution reaction on transition metal (M = Fe, Co, Ni) phosphide pre-catalysts. Chemical Science, 2018, 9, 3470-3476.	3.7	443
56	Boosting the hydrogen evolution performance of ruthenium clusters through synergistic coupling with cobalt phosphide. Energy and Environmental Science, 2018, 11, 1819-1827.	15.6	350
57	Template-Free Synthesis of Hollow Iron Phosphide–Phosphate Composite Nanotubes for Use as Active and Stable Oxygen Evolution Electrocatalysts. ACS Applied Nano Materials, 2018, 1, 617-624.	2.4	66
58	Conformal and continuous deposition of bifunctional cobalt phosphide layers on p-silicon nanowire arrays for improved solar hydrogen evolution. Nano Research, 2018, 11, 4823-4835.	5.8	28
59	Highly-ordered silicon nanowire arrays for photoelectrochemical hydrogen evolution: an investigation on the effect of wire diameter, length and inter-wire spacing. Sustainable Energy and Fuels, 2018, 2, 978-982.	2.5	31
60	A low temperature hydrothermal synthesis of delafossite CuCoO <sub>2</sub> as an efficient electrocatalyst for the oxygen evolution reaction in alkaline solutions. Inorganic Chemistry Frontiers, 2018, 5, 183-188.	3.0	58
61	Hollow cobalt phosphide octahedral pre-catalysts with exceptionally high intrinsic catalytic activity for electro-oxidation of water and methanol. Journal of Materials Chemistry A, 2018, 6, 20646-20652.	5.2	95
62	Cluster Beam Deposition of Ultrafine Cobalt and Ruthenium Clusters for Efficient and Stable Oxygen Evolution Reaction. ACS Applied Energy Materials, 2018, 1, 3013-3018.	2.5	29
63	Ruthenium Cobalt Phosphide Hybrid Clusters with Exceptional Hydrogen Evolution Performance in Both Acidic and Alkaline Electrolytes. ECS Meeting Abstracts, 2018, , .	0.0	0
64	Atomic-layer-deposited ultrafine MoS <sub>2</sub> nanocrystals on cobalt foam for efficient and stable electrochemical oxygen evolution. Nanoscale, 2017, 9, 2711-2717.	2.8	88
65	Vapor–solid synthesis of monolithic single-crystalline CoP nanowire electrodes for efficient and robust water electrolysis. Chemical Science, 2017, 8, 2952-2958.	3.7	162
66	One‣tep Fabrication of Monolithic Electrodes Comprising Co <sub>9</sub> S <sub>8</sub> Particles Supported on Cobalt Foam for Efficient and Durable Oxygen Evolution Reaction. Chemistry - A European Journal, 2017, 23, 8749-8755.	1.7	64
67	Hydrothermal Synthesis of Monolithic Co <sub>3</sub> Se <sub>4</sub> Nanowire Electrodes for Oxygen Evolution and Overall Water Splitting with High Efficiency and Extraordinary Catalytic Stability. Advanced Energy Materials, 2017, 7, 1602579.	10.2	267
68	Tunable Pseudocapacitance in 3D TiO <sub>2â^'î´</sub> Nanomembranes Enabling Superior Lithium Storage Performance. ACS Nano, 2017, 11, 821-830.	7.3	124
69	Vertically Aligned Porous Nickel(II) Hydroxide Nanosheets Supported on Carbon Paper with Longâ€Term Oxygen Evolution Performance. Chemistry - an Asian Journal, 2017, 12, 543-551.	1.7	118
70	Self-supported Co-Ni-P ternary nanowire electrodes for highly efficient and stable electrocatalytic hydrogen evolution in acidic solution. Catalysis Today, 2017, 287, 122-129.	2.2	105
71	Bifunctional Nickel Phosphide Nanocatalysts Supported on Carbon Fiber Paper for Highly Efficient and Stable Overall Water Splitting. Advanced Functional Materials, 2016, 26, 4067-4077.	7.8	591
72	Passivation of hematite nanorod photoanodes with a phosphorus overlayer for enhanced photoelectrochemical water oxidation. Nanotechnology, 2016, 27, 375401.	1.3	28

#	Article	IF	CITATIONS
73	From water reduction to oxidation: Janus Co-Ni-P nanowires as high-efficiency and ultrastable electrocatalysts for over 3000Âh water splitting. Journal of Power Sources, 2016, 330, 156-166.	4.0	190
74	Facile synthesis of hierarchical β-LiFePO4and its phase transformation to electrochemically active α-LiFePO4for Li-ion batteries. CrystEngComm, 2016, 18, 7707-7714.	1.3	6
75	Facile synthesis of iron phosphide nanorods for efficient and durable electrochemical oxygen evolution. Chemical Communications, 2016, 52, 8711-8714.	2.2	168
76	Optimization of filler type within poly(vinylidene fluoride-co-trifluoroethylene) composite separator membranes for improved lithium-ion battery performance. Composites Part B: Engineering, 2016, 96, 94-102.	5.9	48
77	Efficient and durable electrochemical hydrogen evolution using cocoon-like MoS2 with preferentially exposed edges. International Journal of Hydrogen Energy, 2016, 41, 9344-9354.	3.8	74
78	Fast fabrication of self-supported porous nickel phosphide foam for efficient, durable oxygen evolution and overall water splitting. Journal of Materials Chemistry A, 2016, 4, 5639-5646.	5.2	224
79	Self-Supported Three-Dimensional Macroporous Nickel Phosphide Electrodes for Overall Electrochemical Water Splitting. ECS Meeting Abstracts, 2016, , .	0.0	0
80	Deep dissolution system for high-efficiency wells exploration in carbonate karst reservoir: A case study in the Tazhong area. , 2016, , .		0
81	Construction of efficient-sensitive factor for complex carbonate reservoirs and its applications. Journal of Geophysics and Engineering, 2015, 12, 887-896.	0.7	1
82	Porous Si Nanowires from Cheap Metallurgical Silicon Stabilized by a Surface Oxide Layer for Lithium Ion Batteries. Advanced Functional Materials, 2015, 25, 6701-6709.	7.8	173
83	Oneâ€Step Synthesis of Selfâ€Supported Nickel Phosphide Nanosheet Array Cathodes for Efficient Electrocatalytic Hydrogen Generation. Angewandte Chemie - International Edition, 2015, 54, 8188-8192.	7.2	494
84	One‣tep Synthesis of Self‣upported Nickel Phosphide Nanosheet Array Cathodes for Efficient Electrocatalytic Hydrogen Generation. Angewandte Chemie, 2015, 127, 8306-8310.	1.6	86
85	Silicon nanowire arrays coupled with cobalt phosphide spheres as low-cost photocathodes for efficient solar hydrogen evolution. Chemical Communications, 2015, 51, 10742-10745.	2.2	54
86	Binder-free electrodes consisting of porous NiO nanofibers directly electrospun on nickel foam for high-rate supercapacitors. Materials Letters, 2015, 144, 114-118.	1.3	75
87	Direct solvothermal phosphorization of nickel foam to fabricate integrated Ni <sub>2</sub> P-nanorods/Ni electrodes for efficient electrocatalytic hydrogen evolution. Chemical Communications, 2015, 51, 6738-6741.	2.2	149
88	Up-scaling the synthesis of Cu2O submicron particles with controlled morphologies for solar H2 evolution from water. Journal of Colloid and Interface Science, 2015, 456, 219-227.	5.0	20
89	Carbonate reservoirs dominated by secondary storage space: Key issues and technical strategy. The Leading Edge, 2015, 34, 90-98.	0.4	9
90	Efficient water oxidation using α-Fe2O3 thin films conformally coated on vertically aligned titania nanotube arrays by atomic layer deposition. Materials Letters, 2015, 159, 284-288.	1.3	12

#	Article	IF	CITATIONS
91	Amorphous oxygen-rich molybdenum oxysulfide Decorated p-type silicon microwire Arrays for efficient photoelectrochemical water reduction. Nano Energy, 2015, 16, 130-142.	8.2	85
92	Design and Synthesis of Highly Active Al–Ni–P Foam Electrode for Hydrogen Evolution Reaction. ACS Catalysis, 2015, 5, 6503-6508.	5.5	98
93	Highâ€Performance Liâ€O <sub>2</sub> Batteries with Trilayered Pd/MnO <i><sub>x</sub></i> /Pd Nanomembranes. Advanced Science, 2015, 2, 1500113.	5.6	55
94	Poly(vinylidene fluoride-co-chlorotrifluoroethylene) (PVDF-CTFE) lithium-ion battery separator membranes prepared by phase inversion. RSC Advances, 2015, 5, 90428-90436.	1.7	39
95	Platinum nanoparticle interlayer promoted improvement in photovoltaic performance of silicon/PEDOT:PSS hybrid solar cells. Materials Chemistry and Physics, 2015, 149-150, 309-316.	2.0	11
96	Silicon nanowires fabricated by porous gold thin film assisted chemical etching and their photoelectrochemical properties. Materials Letters, 2014, 125, 28-31.	1.3	14
97	Threeâ€Dimensionally "Curved―NiO Nanomembranes as Ultrahigh Rate Capability Anodes for Liâ€ŀon Batteries with Long Cycle Lifetimes. Advanced Energy Materials, 2014, 4, 1300912.	10.2	263
98	Hierarchically Designed SiOx/SiOy Bilayer Nanomembranes as Stable Anodes for Lithium Ion Batteries. Advanced Materials, 2014, 26, 4527-4532.	11.1	141
99	Ordered arrays of tilted silicon nanobelts with enhanced solar hydrogen evolution performance. Nanoscale, 2014, 6, 2097.	2.8	8
100	Improved photo-stability of silicon nanobelt arrays by atomic layer deposition for efficient photocatalytic hydrogen evolution. Journal of Power Sources, 2014, 268, 677-682.	4.0	14
101	Multifunctional Ni/NiO hybrid nanomembranes as anode materials for high-rate Li-ion batteries. Nano Energy, 2014, 9, 168-175.	8.2	268
102	Free-standing Fe2O3 nanomembranes enabling ultra-long cycling life and high rate capability for Li-ion batteries. Scientific Reports, 2014, 4, 7452.	1.6	83
103	Nickel foam supported mesoporous MnO2 nanosheet arrays with superior lithium storage performance. Chemical Communications, 2013, 49, 8459.	2.2	108
104	Nano-aggregates of cobalt nickel oxysulfide as a high-performance electrode material for supercapacitors. Nanoscale, 2013, 5, 11615.	2.8	66
105	Direct growth of mesoporous MnO 2 nanosheet arrays on nickel foam current collectors for high-performance pseudocapacitors. Journal of Power Sources, 2013, 243, 676-681.	4.0	138
106	Porous Co16S16O96 nanosheets as a new electrode material for use inÂsupercapacitors. Journal of Power Sources, 2013, 239, 24-29.	4.0	7
107	Novel Threeâ€Dimensional Nanoporous Alumina as a Template for Hierarchical TiO <sub>2</sub> Nanotube Arrays. Small, 2013, 9, 1025-1029.	5.2	42
108	Hierarchical Structures: Novel Threeâ€Đimensional Nanoporous Alumina as a Template for Hierarchical TiO <sub>2</sub> Nanotube Arrays (Small 7/2013). Small, 2013, 9, 1120-1120.	5.2	1

#	Article	IF	CITATIONS
109	A noise-resistant density inversion algorithm and its application on high efficiency well selection for complex carbonate reservoir. , 2013, , .		6
110	Studying heterogeneity and anisotropy via numerical and physical modeling. The Leading Edge, 2012, 31, 190-196.	0.4	14
111	Atomic Layer Deposition Assisted Template Approach for Electrochemical Synthesis of Au Crescent-Shaped Half-Nanotubes. ACS Nano, 2011, 5, 788-794.	7.3	31
112	Fabrication and characterization of extended arrays of Ag2S/Ag nanodot resistive switches. Applied Physics Letters, 2011, 98, 243109.	1.5	41
113	Spontaneous Phase and Morphology Transformations of Anodized Titania Nanotubes Induced by Water at Room Temperature. Nano Letters, 2011, 11, 3649-3655.	4.5	188
114	The fabrication of nanoporous Pt-based multimetallic alloy nanowires and their improved electrochemical durability. Nanotechnology, 2011, 22, 105604.	1.3	29
115	Seismic attributes and integrated prediction of fractured and caved carbonate reservoirs in the Tarim Basin, China. Petroleum Science, 2011, 8, 455-461.	2.4	12
116	Quasi-radial growth of metal tube on si nanowires template. Nanoscale Research Letters, 2011, 6, 165.	3.1	29
117	Lowâ€Platinum ontent Quaternary PtCuCoNi Nanotubes with Markedly Enhanced Oxygen Reduction Activity. Angewandte Chemie - International Edition, 2011, 50, 2729-2733.	7.2	110
118	Regulated Oxidation of Nickel in Multisegmented Nickel–Platinum Nanowires: An Entry to Wavy Nanopeapods. Angewandte Chemie - International Edition, 2011, 50, 10855-10858.	7.2	21
119	Fabrication of diameter-modulated and ultrathin porous nanowires in anodic aluminum oxide templates. Electrochimica Acta, 2011, 56, 4972-4979.	2.6	105
120	Bubble polarization domain patterns in periodically ordered epitaxial ferroelectric nanodot arrays. Journal of Applied Physics, 2011, 110, .	1.1	13
121	A novel synthesis of ultrathin CoPt3 nanowires by dealloying larger diameter Co99Pt1 nanowires and subsequent stress-induced crack propagation. Electrochemistry Communications, 2010, 12, 835-838.	2.3	8
122	Synthesis of silicon nanotubes with cobalt silicide ends using anodized aluminum oxide template. Nanotechnology, 2010, 21, 055603.	1.3	14
123	Capillary Condensation and Evaporation in Alumina Nanopores with Controlled Modulations. Langmuir, 2010, 26, 11894-11898.	1.6	57
124	Metal-assisted electrochemical etching of silicon. Nanotechnology, 2010, 21, 465301.	1.3	96
125	Continuous Fabrication of Free-Standing TiO <sub>2</sub> Nanotube Array Membranes with Controllable Morphology for Depositing Interdigitated Heterojunctions. Chemistry of Materials, 2010, 22, 6656-6664.	3.2	109
126	Microstructure and Properties of Well-Ordered Multiferroic Pb(Zr,Ti)O <sub>3</sub> /CoFe <sub>2</sub> O <sub>4</sub> Nanocomposites. ACS Nano, 2010, 4, 1099-1107.	7.3	86

#	Article	IF	CITATIONS
127	Microstructure, electrocatalytic and sensing properties of nanoporous Pt46Ni54 alloy nanowires fabricated by mild dealloying. Journal of Materials Chemistry, 2010, 20, 5621.	6.7	79
128	From Co/Pt multilayered nanowires to Co–Pt alloy nanowires: structural and magnetic evolutions with annealing temperatures. Journal Physics D: Applied Physics, 2009, 42, 205002.	1.3	13
129	Highâ€Density Periodically Ordered Magnetic Cobalt Ferrite Nanodot Arrays by Templateâ€Assisted Pulsed Laser Deposition. Advanced Functional Materials, 2009, 19, 3450-3455.	7.8	74
130	Nanoporous Ptâ^'Co Alloy Nanowires: Fabrication, Characterization, and Electrocatalytic Properties. Nano Letters, 2009, 9, 4352-4358.	4.5	377
131	Vortex Polarization States in Nanoscale Ferroelectric Arrays. Nano Letters, 2009, 9, 1127-1131.	4.5	197
132	An integrated study on fractured and cavernous carbonate reservoir prediction — multiâ€attribute optimization discriminant analysis for Tarim Basin. , 2009, , .		0
133	Synthesis, characterization, photoluminescence and ferroelectric properties of PbTiO3 nanotube arrays. Materials Science and Engineering B: Solid-State Materials for Advanced Technology, 2008, 149, 41-46.	1.7	44
134	Tailorâ€Made Inorganic Nanopeapods: Structural Design of Linear Noble Metal Nanoparticle Chains. Angewandte Chemie - International Edition, 2008, 47, 7004-7008.	7.2	61
135	Inside Cover: Tailor-Made Inorganic Nanopeapods: Structural Design of Linear Noble Metal Nanoparticle Chains (Angew. Chem. Int. Ed. 37/2008). Angewandte Chemie - International Edition, 2008, 47, 6926-6926.	7.2	0
136	Innentitelbild: Tailor-Made Inorganic Nanopeapods: Structural Design of Linear Noble Metal Nanoparticle Chains (Angew. Chem. 37/2008). Angewandte Chemie, 2008, 120, 7032-7032.	1.6	0
137	Microstructure and temperature-dependent magnetic properties of Co/Pt multilayered nanowires. Chemical Physics Letters, 2008, 466, 165-169.	1.2	26
138	Extended Arrays of Vertically Aligned Sub-10 nm Diameter [100] Si Nanowires by Metal-Assisted Chemical Etching. Nano Letters, 2008, 8, 3046-3051.	4.5	317
139	Enhanced ionic conductivity of AgI nanowires/AAO composites fabricated by a simple approach. Nanotechnology, 2008, 19, 495706.	1.3	18
140	Fabrication and characterization of a flow-through nanoporous gold nanowire/AAO composite membrane. Nanotechnology, 2008, 19, 335604.	1.3	71
141	Highly Efficient Direct Electrodeposition of Coâ^'Cu Alloy Nanotubes in an Anodic Alumina Template. Journal of Physical Chemistry C, 2008, 112, 2256-2261.	1.5	52
142	General Assembly Method for Linear Metal Nanoparticle Chains Embedded in Nanotubes. Nano Letters, 2008, 8, 3221-3225.	4.5	60
143	Growth of ultrafine ZnS nanowires. Nanotechnology, 2007, 18, 145607.	1.3	18
144	Large-scale synthesis and optical behaviors of ZnO tetrapods. Applied Physics Letters, 2007, 90, 153116.	1.5	44

#	Article	IF	CITATIONS
145	Secondary growth of small ZnO tripodlike arms on the end of nanowires. Applied Physics Letters, 2007, 91, 013106.	1.5	5
146	A simple route to scalable fabrication of perfectly ordered ZnO nanorod arrays. Nanotechnology, 2007, 18, 405303.	1.3	42
147	Directly Synthesized Strong, Highly Conducting, Transparent Single-Walled Carbon Nanotube Films. Nano Letters, 2007, 7, 2307-2311.	4.5	334
148	Batchwise Growth of Silica Cone Patterns via Self-Assembly of Aligned Nanowires. Small, 2007, 3, 444-450.	5.2	10
149	Patterned anodic aluminium oxide fabricated with a Ta mask. Nanotechnology, 2006, 17, 35-39.	1.3	16
150	Growth Mechanism, Photoluminescence, and Field-Emission Properties of ZnO Nanoneedle Arrays. Journal of Physical Chemistry B, 2006, 110, 8566-8569.	1.2	83
151	Structural, Magnetic, and Magnetoresistive Properties of Electrodeposited Ni5Zn21Alloy Nanowires. Journal of Physical Chemistry B, 2006, 110, 20158-20165.	1.2	9
152	Periodic ZnO Nanorod Arrays Defined by Polystyrene Microsphere Self-Assembled Monolayers. Nano Letters, 2006, 6, 2375-2378.	4.5	130
153	Temperature Dependence of the Raman Spectra of Individual Carbon Nanotubes. Journal of Physical Chemistry B, 2006, 110, 1206-1209.	1.2	53
154	The growth of carbon nanostructures in the channels of aligned carbon nanotubes. Carbon, 2006, 44, 1310-1313.	5.4	6
155	Human fibrinogen adsorption onto single-walled carbon nanotube films. Colloids and Surfaces B: Biointerfaces, 2006, 49, 66-70.	2.5	24
156	Studies on silver nanodecahedrons synthesized by PVP-assisted N,N-dimethylformamide (DMF) reduction. Journal of Crystal Growth, 2006, 289, 376-380.	0.7	113
157	Structure and electrical characteristics of Nb-doped SrTiO3 substrates. Science Bulletin, 2006, 51, 2035-2037.	1.7	11
158	Large-Scale Synthesis of Rings of Bundled Single-Walled Carbon Nanotubes by Floating Chemical Vapor Deposition. Advanced Materials, 2006, 18, 1817-1821.	11.1	57
159	Electrochemical fabrication and structure of NixZn1â^'xalloy nanowires. Nanotechnology, 2006, 17, 19-24.	1.3	18
160	Efficiently producing single-walled carbon nanotube rings and investigation of their field emission properties. Nanotechnology, 2006, 17, 2355-2361.	1.3	16
161	Template synthesis, characterization and magnetic property of Fe nanowires-filled amorphous carbon nanotubes array. Journal Physics D: Applied Physics, 2006, 39, 3939-3944.	1.3	10
162	Conformal conversion from helical hexagonal InN microtubes to In2O3 counterparts. Applied Physics Letters, 2006, 89, 093112.	1.5	7

#	Article	IF	CITATIONS
163	The influence of hydrogen on the growth of gallium catalyzed silicon oxide nanowires. Journal of Physics and Chemistry of Solids, 2005, 66, 701-705.	1.9	7
164	Silver nanowires with five-fold symmetric cross-section. Journal of Crystal Growth, 2005, 276, 606-612.	0.7	107
165	Surface-enhanced resonant Raman spectroscopy (SERRS) of single-walled carbon nanotubes absorbed on the Ag-coated anodic aluminum oxide (AAO) surface. Physica E: Low-Dimensional Systems and Nanostructures, 2005, 27, 469-473.	1.3	2
166	Surface-enhanced Raman scattering from the individual metallic single-walled carbon nanotubes. Physica E: Low-Dimensional Systems and Nanostructures, 2005, 28, 360-364.	1.3	5
167	Bulk-quantity synthesis of single-crystalline indium nitride nanobelts. Chemical Physics Letters, 2005, 411, 361-365.	1.2	11
168	Synthesis of LongIndium Nitride Nanowires with Uniform Diameters in Large Quantities. Small, 2005, 1, 1004-1009.	5.2	47
169	Three-dimensional micro- and nanometre composite aluminium patterns. Chinese Physics B, 2005, 14, 1471-1476.	1.3	3
170	Growth of ZnO hexagonal nanoprisms. Nanotechnology, 2005, 16, 2665-2669.	1.3	50
171	Template-free synthesis of helical hexagonal microtubes of indium nitride. Applied Physics Letters, 2005, 87, 063109.	1.5	32
172	Effects of donor concentration on the electrical properties of Nb-doped BaTiO3 thin films. Journal of Applied Physics, 2005, 97, 054102.	1.1	36
173	Anodizing Behavior of Aluminum Foil Patterned with SiO[sub 2] Mask. Journal of the Electrochemical Society, 2005, 152, B411.	1.3	7
174	Temperature effect on carrier transport characteristics in SrTiO3â^`î´/Si p-n heterojunction. Applied Physics Letters, 2005, 86, 123502.	1.5	31
175	Low-Temperature Growth and Photoluminescence Property of ZnS Nanoribbons. Journal of Physical Chemistry B, 2005, 109, 18352-18355.	1.2	53
176	Growth mechanism of silver nanowires synthesized by polyvinylpyrrolidone-assisted polyol reduction. Journal Physics D: Applied Physics, 2005, 38, 1061-1067.	1.3	147
177	Structural phase transitions of BaNbxTi1â^'xO3(0.0⩽x⩽0.5) thin films. Journal of Applied Physics, 2004, 9 3404-3407.	6 <sub>1.1</sub>	10
178	Synthesis, optical, and magnetic properties of Zn1â^'xMnxS nanowires grown by thermal evaporation. Journal of Crystal Growth, 2004, 271, 403-408.	0.7	49
179	Multidimensional magnesium oxide nanostructures with cone-shaped branching. Solid State Communications, 2004, 131, 485-488.	0.9	11
180	Synthesis and characterization of a large amount of branched Ni2Si nanowires. Applied Physics A: Materials Science and Processing, 2004, 79, 1853-1856.	1.1	33

#	Article	IF	CITATIONS
181	Direct Synthesis of a Macroscale Single-Walled Carbon Nanotube Non-Woven Material. Advanced Materials, 2004, 16, 1529-1534.	11.1	131
182	Growth of SnO 2 nanowires with uniform branched structures. Solid State Communications, 2004, 130, 89-94.	0.9	148
183	Synthesis, structure, and photoluminescence of Zn2SnO4 single-crystal nanobelts and nanorings. Solid State Communications, 2004, 131, 435-440.	0.9	102
184	Growth and characterization of axially periodic Zn2SnO4 (ZTO) nanostructures. Journal of Crystal Growth, 2004, 267, 177-183.	0.7	90
185	The intrinsic temperature effect of Raman spectra of double-walled carbon nanotubes. Chemical Physics Letters, 2004, 396, 372-376.	1.2	23
186	Structural properties and spin–phonon coupling effect of La1â^'xTexMnO3 thin films. Applied Physics Letters, 2004, 85, 3172-3174.	1.5	18
187	Random Networks of Single-Walled Carbon Nanotubes. Journal of Physical Chemistry B, 2004, 108, 10751-10753.	1.2	30
188	Evidence for the Monolayer Assembly of Poly(vinylpyrrolidone) on the Surfaces of Silver Nanowires. Journal of Physical Chemistry B, 2004, 108, 12877-12881.	1.2	248
189	Synthesis, characterization and self-assembly of silver nanowires. Chemical Physics Letters, 2003, 380, 146-149.	1.2	95
190	Producing cleaner double-walled carbon nanotubes in a floating catalyst system. Carbon, 2003, 41, 2607-2611.	5.4	27
191	Characterization of zinc oxide crystal nanowires grown by thermal evaporation of ZnS powders. Chemical Physics Letters, 2003, 371, 337-341.	1.2	47
192	A simple large-scale synthesis of coaxial nanocables: silicon carbide sheathed with silicon oxide. Chemical Physics Letters, 2003, 375, 269-272.	1.2	22
193	H2-assisted control growth of Si nanowires. Journal of Crystal Growth, 2003, 257, 69-74.	0.7	6
194	Formation of ZnS nanostructures by a simple way of thermal evaporation. Journal of Crystal Growth, 2003, 258, 225-231.	0.7	27
195	Temperature dependence of resonant Raman scattering in double-wall carbon nanotubes. Applied Physics Letters, 2003, 82, 3098-3100.	1.5	69
196	Resonant Raman scattering of double wall carbon nanotubes prepared by chemical vapor deposition method. Journal of Applied Physics, 2003, 94, 5715-5719.	1.1	14
197	Characteristics of LaAlO3/Si(100) deposited under various oxygen pressures. Journal of Applied Physics, 2003, 93, 533-536.	1.1	70
198	Optical properties ofp-type In-doped SrTiO3 thin films. Journal of Applied Physics, 2003, 94, 4558-4562.	1.1	30